

# Stable, Fast and Accurate: Kernelized Attention with Relative Positional Encoding

Shengjie Luo<sup>1\*</sup>, Shanda Li<sup>2\*</sup>, Tianle Cai<sup>3</sup>, Di He<sup>5†</sup>,  
 Dinglan Peng<sup>4</sup>, Shuxin Zheng<sup>5†</sup>, Guolin Ke<sup>5</sup>, Liwei Wang<sup>1,2</sup>, Tie-Yan Liu<sup>5</sup>

<sup>1</sup>Center for Data Science, Peking University

<sup>2</sup>Key Laboratory of Machine Perception, MOE, School of EECS, Peking University

<sup>3</sup>Princeton University    <sup>4</sup>University of Science and Technology of China    <sup>5</sup>Microsoft Research  
 luosj@stu.pku.edu.cn, lishanda@pku.edu.cn,  
 tianle.cai@princeton.edu, pengdinglan@mail.ustc.edu.cn,  
 {dihe, shuz, guoke, tyliu}@microsoft.com, wanglw@pku.edu.cn

## Abstract

The attention module, which is a crucial component in Transformer, cannot scale efficiently to long sequences due to its quadratic complexity. Many works focus on approximating the dot-then-exponentiate softmax function in the original attention, leading to sub-quadratic or even linear-complexity Transformer architectures. However, we show that these methods cannot be applied to more powerful attention modules that go beyond the dot-then-exponentiate style, e.g., Transformers with relative positional encoding (RPE). Since in many state-of-the-art models, relative positional encoding is used as default, designing efficient Transformers that can incorporate RPE is appealing. In this paper, we propose a novel way to accelerate attention calculation for Transformers with RPE on top of the kernelized attention. Based upon the observation that relative positional encoding forms a Toeplitz matrix, we mathematically show that kernelized attention with RPE can be calculated efficiently using Fast Fourier Transform (FFT). With FFT, our method achieves  $\mathcal{O}(n \log n)$  time complexity. Interestingly, we further demonstrate that properly using relative positional encoding can mitigate the training instability problem of vanilla kernelized attention. On a wide range of tasks, we empirically show that our models can be trained from scratch without any optimization issues. The learned model performs better than many efficient Transformer variants and is faster than standard Transformer in the long-sequence regime.

## 1 Introduction

Transformer [45] has achieved tremendous success on a variety of tasks in natural language processing [34, 9, 50], computer vision [2, 10, 42] and speech [13]. Despite the great success, Transformers are usually inefficient in modeling long-sequence input since the key component—the attention module—needs to calculate pairwise correlations between all the positions, which comes with quadratic time and memory cost with respect to the sequence length  $n$ .

To reduce the cost, many works focus on approximating the dot-then-exponentiate function in the attention module of the original Transformer [41]. Most works can be roughly categorized into three classes: sparse attention [3, 33, 30, 15, 21, 46, 7], low-rank approximation-based attention [49, 48] and kernelized attention [17, 32, 4]. Sparse attention variants design either pre-defined [3, 33, 30, 15] or learnable patterns [21, 46, 7] to reduce the amount of the key-value pairs that each

\*Equal contribution.

†Correspondence to: Di He <dihe@microsoft.com> and Shuxin Zheng <shuz@microsoft.com>.

query needs to attend to. Low-rank approximation-based attention variants project the key matrix into a length-agnostic low-dimensional space [48], or use Nyström approximation [49] to reduce the quadratic dependency on sequence length. The kernelized attention is first developed in [44, 17], which introduces a kernel view on the dot-then-exponentiate softmax function and comes up with a linear attention mechanism. Followed-up works [32, 4] theoretically investigate the choices of different kernel feature maps and propose several random feature maps that achieve much better performance on various applications.

However, in recently developed Transformers, the attention mechanism is designed to be more complicated than dot-then-exponentiation. For example, the relative positional encoding (RPE) [38, 35] has become standard in state-of-the-art models [35, 18, 14]: Besides using the dot-products between queries and keys, RPE incorporates a position-correlation matrix in the softmax exponentiation to encode the distance between any two positions. With RPE, Transformers can effectively capture the relative word orders and achieve superior performance on various tasks. As Transformer with RPE is more powerful, one may wonder whether the model can be still approximated by directly applying previous acceleration approaches.

Unfortunately, we mathematically show that such a term expands the expressiveness of dot-then-exponentiation, i.e., for some attention with RPE, there exists no dot-then-exponentiate function that can represent it. Therefore, previous approaches cannot be directly applied to approximate Transformers with RPE and obtain non-trivial speed-up. In this paper, we develop a novel attention computation that achieves an almost-linear speed-up rate for Transformer with RPE. We build our method on top of the kernelized attention in [4, 32]. The kernelized attention method replaces the dot-then-exponentiate attention by a simple matrix multiplication between the kernelized features of queries and key-value pairs. When taking RPE into the kernelized attention, one can naively multiply the  $n \times n$  RPE position-correlation matrix with kernelized feature matrices, which leads to a trivial quadratic time cost. While interestingly, we find that the elements in the RPE position-correlation matrix are determined by the relative distance between positions, and this matrix is precisely a Toeplitz matrix. In numerical linear algebra, it is well-known that multiplication between a Toeplitz matrix and row vectors can be accelerated using Fast Fourier Transform (FFT). And by using FFT, we can obtain a fast attention computation with  $\mathcal{O}(n \log n)$  time cost.

Beyond the efficiency, we also find that our method that incorporates RPE into kernelized attention can also stabilize the training of such models. As demonstrated by several works [16, 4], although these kernelized attention methods have theoretical guarantees to approximate the softmax attention, they face optimization issues and will diverge when training from scratch for large-scale tasks. This significantly limits the practical impact of the model as we have to train a standard Transformer first and convert it to kernelized attention with finetuning. We first shed light upon the reason for this phenomenon by proving that these kernelized attentions have an unacceptable variance when the  $\ell_2$  norms of queries and keys are large. However, queries and keys with large norms usually appear during training, leading to optimization instability or sub-optimal solutions. When incorporating RPE, we can properly normalize queries and keys to obtain a “low-variance” attention, making the training stable. Since the value range of the relative positional encodings is not constrained, the whole model can still have enough capacity to achieve good performance.

We conduct experiments on a wide range of tasks spanning language pre-training, machine translation and image classification. On all the tasks, we show that our model can be trained from scratch stably, outperforms other competitive efficient models, and is faster than the standard Transformer in the long-sequence regime.

## 2 Preliminary

### 2.1 Attention Module and its Kernel View

The attention module is one of the key components in the Transformer [45, 9]. It is usually formulated as querying a dictionary with key-value pairs, e.g.,  $\text{Attention}(Q, K, V) = \text{softmax}\left(\frac{QW^Q(KW^K)^\top}{\sqrt{d}}\right)VW^V$ , where  $d$  is the dimensionality of the hidden representations.  $Q$  (Query),  $K$  (Key),  $V$  (Value) are specified as the hidden representations of the previous layer and  $W^Q, W^K$  and  $W^V$  are projection matrices for any specific head.

To be more concrete, we denote  $x = (x_1, x_2 \dots, x_n)$  as the input to the attention module, where  $n$  is the length of the sequence and  $x_i \in \mathbb{R}^d$  is a row vector denoting the contextual representation of the token at position  $i$ . Denote  $z = (z_1, z_2 \dots, z_n)$  as the output. Then the attention module can be written as

$$z_i = \sum_{j=1}^n \frac{\exp(\alpha_{ij})}{\sum_{j'=1}^n \exp(\alpha_{ij'})} (x_j W^V), \text{ where } \alpha_{ij} = \frac{1}{\sqrt{d}} (x_i W^Q) (x_j W^K)^\top. \quad (1)$$

As we can see, the calculation of attention for each position requires  $\mathcal{O}(n)$  time and memory cost. Thus, the time and memory cost for the whole sequence is  $\mathcal{O}(n^2)$ , which impedes the attention mechanism scaling to long sequences. Recently, [44, 17] introduce a kernel view on the attention mechanism and derive a general kernelized attention framework as follows:

$$z_i = \sum_{j=1}^n \frac{\kappa(x_i W^Q, x_j W^K)}{\sum_{j'=1}^n \kappa(x_i W^Q, x_{j'} W^K)} (x_j W^V), \quad (2)$$

where  $\kappa(\cdot, \cdot) : \mathbb{R}^d \times \mathbb{R}^d \rightarrow \mathbb{R}$  is any positive-definite kernel measuring the pairwise similarity. Based on this kernel view, the attention mechanism can be alternatively modeled as a linear dot-product of kernelized features:

$$z_i = \sum_{j=1}^n \frac{\phi(x_i W^Q) \phi(x_j W^K)^\top}{\sum_{j'=1}^n \phi(x_i W^Q) \phi(x_{j'} W^K)^\top} (x_j W^V) = \frac{\phi(x_i W^Q) \sum_{j=1}^n \phi(x_j W^K)^\top (x_j W^V)}{\phi(x_i W^Q) \sum_{j'=1}^n \phi(x_{j'} W^K)^\top}, \quad (3)$$

where  $\phi(\cdot) : \mathbb{R}^d \rightarrow \mathbb{R}^m$  is the feature map and  $m$  is the dimension of the feature space. Since both  $\sum_{j=1}^n \phi(x_j W^K) (x_j W^V)$  and  $\sum_{j'=1}^n \phi(x_{j'} W^K)$  can be reused for each position, the time and memory complexity of the kernelized attention is reduced to  $\mathcal{O}(n)$ . [17] simply uses  $\text{elu}(\cdot) + 1$  as  $\phi(\cdot)$ . Followed-up works [32, 4] further propose two (randomized) feature maps with which the kernels are unbiased estimators of the dot-then-exponentiate function, therefore achieve similar expressiveness as the standard Transformer. For simplicity, we call the feature maps used in [32] and [4] as Trigonometric Random Feature (TRF) and Positive Random Feature (PRF) respectively:

$$\phi_{TRF}(x) = \frac{\exp(-\frac{\|x\|^2}{2})}{\sqrt{m}} [\sin(w_1 x^\top), \dots, \sin(w_m x^\top), \cos(w_1 x^\top), \dots, \cos(w_m x^\top)], \quad (4)$$

$$\phi_{PRF}(x) = \frac{\exp(-\frac{\|x\|^2}{2})}{\sqrt{m}} [\exp(w_1 x^\top), \dots, \exp(w_m x^\top)], \quad (5)$$

where each vector  $w_i$  is independently sampled from  $N(0, I_d)$ . Our work aims to design an efficient Transformer with relative positional encoding on top of the kernelized attention. Without loss of generality, we use Positive Random Features as the feature map to demonstrate the effectiveness of our approach. Our approach can also be applied to other feature maps such as the Trigonometric Random Features. See Section 4.5 for some ablation studies.

## 2.2 Relative Positional Encoding

Relative Positional Encoding (RPE) is recognized as one of the most successful modifications to the original Transformer model [27]. RPE is first introduced in [38], which suggests that using absolute positional encoding may be ineffective in capturing relative word orders. They propose an embedding matrix in which the values of the elements are determined by the distance between the row index and column index. [35] further proposes a simple yet more effective relative positional encoding, which is popularly used in many recent state-of-the-art Transformers, including [1, 18, 24]. In this model [35], the relative positional encoding is served as a bias term added to the dot-product between queries and keys:

$$\alpha_{ij}^{rel} = \frac{1}{\sqrt{d}} (x_i W^Q) (x_j W^K)^\top + b_{j-i}. \quad (6)$$

For each  $j - i$ ,  $b_{j-i}$  is a learnable scalar and shared across all layers.

### 3 Incorporating RPE into Kernelized Attention

We are curious about whether previous acceleration methods can be directly applied to Transformers with RPE for achieving both speed-up and better accuracy. In this section, we first provide a negative result: We prove that RPE expands the expressiveness of the original attention module. So those efficient approaches that can only approximate dot-then-exponentiate functions *cannot* approximate Transformers with RPE at least in the sense of representation power. To address the problem, we develop new techniques for computing attention with RPE on top of the kernelized attention, and show that we can still obtain non-trivial speed-up using Fast Fourier Transform. Lastly, we study how to stabilize the training of the PRF attention and achieve good performance with the help of RPE. Due to space limitations, we put all the proofs in Appendix B.

#### 3.1 Attention with RPE Goes Beyond the Dot-then-exponentiate Function Class

For simplicity, we study the single-head attention as a demonstration where  $W_{\text{rel}}^Q, W_{\text{rel}}^K \in \mathbb{R}^{d \times d}$ . All the conclusions remain the same for the multi-head attention setting. The following proposition shows that Transformers with RPE are strictly more expressive than those without RPE.

**Proposition 1.** *If  $n > d + 1$ , there exist weight matrices  $W_{\text{rel}}^Q, W_{\text{rel}}^K \in \mathbb{R}^{d \times d}$  and RPE weights  $b_{j-i}$  as in Equation 6, such that there does **not** exist weight matrices  $W_{\text{vanilla}}^Q, W_{\text{vanilla}}^K$  and input vectors  $x_1, \dots, x_n \in \mathbb{R}^d$  that satisfy*

$$\frac{\exp(\alpha_{ij}^{\text{rel}})}{\sum_{k=1}^n \exp(\alpha_{ik}^{\text{rel}})} = \frac{\exp(\alpha_{ij}^{\text{vanilla}})}{\sum_{k=1}^n \exp(\alpha_{ik}^{\text{vanilla}})}, \quad \forall i, j. \quad (7)$$

where

$$\alpha_{ij}^{\text{rel}} = \frac{1}{\sqrt{d}} (x_i W_{\text{rel}}^Q) (x_j W_{\text{rel}}^K)^\top + b_{j-i}; \quad (8)$$

$$\alpha_{ij}^{\text{vanilla}} = \frac{1}{\sqrt{d}} (x_i W_{\text{vanilla}}^Q) (x_j W_{\text{vanilla}}^K)^\top. \quad (9)$$

This theoretical finding is consistent with all empirical observations that Transformers equipped with RPE are more powerful and usually perform better than the original Transformer. At the same time, such a result suggests that Transformers with RPE cannot be well-approximated by techniques developed in the previous works as those methods are under the simple dot-then-exponentiate attention setting. To accelerate Transformers with RPE, new techniques need to be explored.

#### 3.2 Fast Attention Calculation using Fast Fourier Transform

We propose an efficient method that accelerates the computation of attention modules with RPE. The approach is built on top of the kernelized attentions, i.e., Equation 3. When relative positional encoding is further implemented, the kernelized attention will be formulated as:

$$z_i = \frac{\phi(x_i W^Q) \sum_{j=1}^n e^{b_{j-i}} \phi(x_j W^K)^\top (x_j W^V)}{\phi(x_i W^Q) \sum_{j=1}^n e^{b_{j-i}} \phi(x_j W^K)^\top}. \quad (10)$$

From Equation 10, we can see that to calculate the output  $(z_i)_{i=1}^n$ , we need to compute  $D_1 = \left( \sum_{j=1}^n e^{b_{j-i}} \phi(x_j W^K)^\top (x_j W^V) \right)_{i=1}^n$  and  $D_2 = \left( \sum_{j=1}^n e^{b_{j-i}} \phi(x_j W^K) \right)_{i=1}^n$ . To better illustrate the calculation step, we reshape  $D_1, D_2$  into the form where elements are vectorized as row vectors and stacked into matrices:

$$\tilde{D}_1 = \begin{pmatrix} \text{vec} \left( \sum_{j=1}^n e^{b_{j-1}} \phi(x_j W^K)^\top (x_j W^V) \right) \\ \vdots \\ \text{vec} \left( \sum_{j=1}^n e^{b_{j-n}} \phi(x_j W^K)^\top (x_j W^V) \right) \end{pmatrix}, \quad \tilde{D}_2 = \begin{pmatrix} \text{vec} \left( \sum_{j=1}^n e^{b_{j-1}} \phi(x_j W^K)^\top \right) \\ \vdots \\ \text{vec} \left( \sum_{j=1}^n e^{b_{j-n}} \phi(x_j W^K)^\top \right) \end{pmatrix}, \quad (11)$$

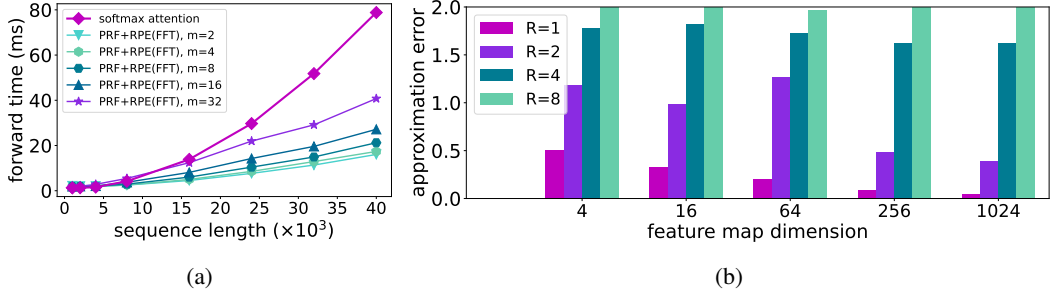


Figure 1: (a). Model forward speed of vanilla Transformer and our model with different feature map dimensions ( $m$ ). (b). Approximation error of PRF with different query/key norms ( $R$ ).

where  $\text{vec}(\cdot)$  denotes vectorization operation. Let  $c_i = e^{b_i}$ .  $\tilde{D}_1, \tilde{D}_2$  can be factorized as the multiplication of two known matrices:

$$\tilde{D}_1 = \begin{pmatrix} c_0 & c_1 & c_2 & \cdots & c_{n-1} \\ c_{-1} & c_0 & c_1 & \cdots & c_{n-2} \\ \vdots & \vdots & \vdots & \ddots & \vdots \\ c_{-(n-1)} & c_{-(n-2)} & c_{-(n-3)} & \cdots & c_0 \end{pmatrix} \begin{pmatrix} \text{vec}(\phi(x_1 W^K)^\top (x_1 W^V)) \\ \text{vec}(\phi(x_2 W^K)^\top (x_2 W^V)) \\ \vdots \\ \text{vec}(\phi(x_n W^K)^\top (x_n W^V)) \end{pmatrix}, \quad (12)$$

$$\tilde{D}_2 = \begin{pmatrix} c_0 & c_1 & c_2 & \cdots & c_{n-1} \\ c_{-1} & c_0 & c_1 & \cdots & c_{n-2} \\ \vdots & \vdots & \vdots & \ddots & \vdots \\ c_{-(n-1)} & c_{-(n-2)} & c_{-(n-3)} & \cdots & c_0 \end{pmatrix} \begin{pmatrix} \text{vec}(\phi(x_1 W^K)^\top) \\ \text{vec}(\phi(x_2 W^K)^\top) \\ \vdots \\ \text{vec}(\phi(x_n W^K)^\top) \end{pmatrix}. \quad (13)$$

Denote  $C = \{c_{j-i}\}_{i,j=1}^n$  as the positional-correlation matrix. It can be easily seen that one can use naive matrix multiplication to obtain  $\tilde{D}_1, \tilde{D}_2$ . But it leads to quadratic time cost with respect to the sequence length  $n$  and makes the advantage of using kernelized attention disappear. Interestingly, we notice that  $C$  is a diagonal-constant matrix in which each descending diagonal from left to right is constant, i.e., a Toeplitz matrix. In numerical linear algebra [11], left multiplying a Toeplitz matrix can be done in  $\mathcal{O}(n \log n)$  time using Fast Fourier Transform (FFT). This fact leads to an efficient algorithm to compute kernelized attention with RPE in  $\mathcal{O}(n \log n)$  time.<sup>3</sup>

We empirically evaluate the forward cost of the kernelized Transformer with RPE using FFT and the standard Transformer. For simplicity, we set the number of heads to 1 and the size of embedding to 64. We use synthetic input sequences with lengths ranging from 1k to 40k. For our model, we experiment with different feature map dimensions. All the experiments are run on a Tesla V100 GPU with 16GB memory for ten trials. The averaged result is shown in Figure 1a. It can be seen that while the forward cost of standard attention becomes much significant on longer sequences, our model still remains efficient (almost linear) in the long-sequence regime.

### 3.3 RPE Enables Stable Training of Kernelized Attention

Recent works [4, 32] show that PRF and TRF attention can approximate the dot-then-exponentiate attention with theoretical guarantees and achieves much better performance than other methods. However, the training of these models is challenging. As demonstrated by several works [16, 4], kernelized attention can hardly be optimized from scratch for large-scale tasks and may even diverge during training. This significantly limits the practical impact of the model as one has to train a standard Transformer first and convert it to the kernelized version. [16] further observed that the model conversion usually leads to a considerable performance drop which suggests that the

<sup>3</sup>One limitation of the proposed method is that it cannot accelerate sequence generation models *during the inference step*. In our approach,  $D_1$  and  $D_2$  need to be pre-computed using FFT for all the queries as a whole. However, in the inference step of the sequence generation, we cannot pre-compute  $D_1$  and  $D_2$  as the tokens are generated on the fly and the FFT operation needs to be used in each time step. But our method can still be used to accelerate the training of the generation model which uses teacher forcing by setting  $b_{i-j} = -\infty$  (i.e.,  $c_{i-j} = 0$ ) when  $i > j$ . We leave how to accelerate the inference step using our method as future work.

approximation seems to be inaccurate. To understand the problem, we start with Lemma 2 below from [4], which analyzes the variance of the softmax-kernel estimation with the PRF feature map.

**Lemma 2** (Variance of the PRF (Lemma 2 in [4])). *For  $\phi_{PRF}$  defined in Equation 5, we have*

$$\text{Var}(\phi(x)\phi(y)^\top) = \frac{1}{m} (\exp(\|x+y\|^2) - 1) \exp(xy^\top)^2. \quad (14)$$

It can be seen from the above lemma that the variance of the estimation is related to the *scale of the queries and keys*. If the scale of the queries and keys is large, the variance will be significant. Our following theorem precisely characterizes that one may need an exponential number of feature map dimensions to obtain a well-approximated PRF kernelized attention. Similar results also hold for the TRF kernel<sup>4</sup>.

**Theorem 3** (Sample Complexity of Approximation). *For a query  $q$  and  $n$  keys  $k_1, \dots, k_n$ , let  $A, \hat{A}$  be the attention score obtained by the standard softmax and the PRF approximation respectively. Assume that  $\ell_2$ -norms of the query and keys are upper-bounded by  $R$ . Then for any  $\varepsilon > 0$ , if feature map dimension  $m = \Theta(\frac{n \exp(4R^2)}{\varepsilon^2 \delta})$ , we have  $\Pr(\|A - \hat{A}\|_1 \geq \varepsilon) \leq \delta$ .*

We also perform numerical simulations to verify the theoretical findings. We set  $d = 64$  as the query/key dimension and independently sample a query vector and 1024 key vectors from the uniform distribution over a  $d$  dimensional unit hypersphere. Therefore, the  $\ell_2$ -norm of the query and the keys we sampled equals one. Denote  $R \geq 1$  as a scaling factor. For each value of  $R$ , we rescale the query and the keys with  $R$  and calculate the softmax score  $A$  and the approximated score  $\hat{A}$  using PRF with different feature map dimensions. We use  $\|A - \hat{A}\|_1$  to quantify the approximation error. The results are shown in Figure 1b. It can be seen that when  $R$  is large, the approximation error is huge and can only be slightly improved as the feature map dimension grows from 4 to 1024. But when  $R = 1$ , the approximation error is small and drops significantly when we increase the feature map dimension. This numerical result is consistent with our theory, which implies that the scale of the queries and keys significantly matters the approximation quality.

Based on the results, we can understand why the model conversion (well-trained standard attention  $\rightarrow$  kernelized attention) usually leads to performance drop as observed in [16]. For a well-trained Transformer, some attention heads generate sharp attention distributions (e.g., attending to the next token [6]). To generate a sharp attention distribution, queries and keys with a large norm are essential. If we convert those attention heads to their kernelized version, the output can be significantly different due to the large variance, and the performance will be poor. Furthermore, queries and keys with a large norm may also be the root cause of the training instability [4]. As discussed in [45], at initialization, the parameters are sampled from Gaussian distribution and unbounded. If the norms of the queries or keys happen to be larger than one, the kernelized attention (forward pass) will have a large variance, leading to a large-variance gradient (backward pass) and making the training unstable.

**Normalized Kernelized Attention with RPE.** A straightforward solution to fix the problem is normalizing queries and keys by their  $\ell_2$  norms<sup>5</sup>, so the variance of the kernelized attention will be well controlled. However, this would bound the dot-products between queries and keys into range  $[-1, 1]$ . Then the attention mechanism can no longer represent sharp distributions, which will hurt the model performance. Fortunately, when equipped with RPE, the model is endowed with the ability to model sharp attention distributions even if the queries and keys are normalized, since relative positional encoding  $b_{j-i}$  remains unbounded. For ease of reference, we call our model Normalized PRF Transformer with RPE and use NPRF-Transformer with RPE for short. A pseudocode implementation is provided in Algorithm 1. In the next section, we will show that

---

<sup>4</sup>In [4], the authors provide a sample complexity bound of the approximation error between the TRF kernel and the dot-then-exponentiate function without considering the denominator term in the softmax. In this paper, we directly provide the sample complexity bound on the approximation error between the PRF-induced attention distribution and the softmax attention distribution.

<sup>5</sup>The TRF paper [32] also proposes to normalize queries and keys. In [32], the normalized queries and keys are multiplied with a Gaussian vector  $w$  which is *rescaled* using a learnable vector  $\sigma \in \mathbb{R}^d$ . This is equivalent to rescaling the normalized  $q$  and  $k$  using  $\sigma$  and then feeding them into  $\phi(\cdot)$ . This doesn't control the norms of queries and keys since the scale of  $\sigma$  can be large, which doesn't address the optimization issue.

---

**Algorithm 1** Efficient Normalized Kernelized Attention with RPE using FFT

---

```

function RPE_NKA(  $Q, K, V, W^Q, W^K, W^V, b = (b_{-(n-1)}, \dots, b_{n-1}), \phi$ ):
    #  $X_i$  denotes the  $i$ -th element of  $X$ 
     $Q \leftarrow \left( \frac{Q_i W^Q}{\|Q_i W^Q\|_2} \right)_{i=1}^n, K \leftarrow \left( \frac{K_i W^K}{\|K_i W^K\|_2} \right)_{i=1}^n, V \leftarrow (V_i W^V)_{i=1}^n$ 
     $c \leftarrow \exp(b), A_1 \leftarrow (\phi(K_i)^\top V_i)_{i=1}^n, A_2 \leftarrow (\phi(K_i)^\top)_{i=1}^n$ 
    # FFTMatrixMul() is an FFT-based algorithm for multiplying a Toeplitz matrix as in Eq. (12), (13). We omit the reshaping steps and assume the second input variable and the output have the same shape.
     $D_1 \leftarrow \text{FFTMatrixMul}(c, A_1), D_2 \leftarrow \text{FFTMatrixMul}(c, A_2)$ 
     $X \leftarrow \left( \frac{\phi(Q_i) D_{1,i}}{\phi(Q_i) D_{2,i}} \right)_{i=1}^n$ 
    return  $X$ .
end

```

---

Table 1: GLUE scores on dev set. “\*” indicates the best performance.

Method	Complexity	CoLA	RTE	MRPC	STS-B	MNLI	QNLI	QQP	SST-2	AVG
<i>Finetune from RoBERTa-base</i>										
SMYRF [7]	$\mathcal{O}(n \log n)$	58.8	68.6	87.7	89.7	85.0	91.1	89.7	93.2	83.0
FCA [46]	$\mathcal{O}(n)$	59.8	49.8	43.6	78.9	79.4	74.6	89.4	94.4	71.2
Improved FCA [46]	$\mathcal{O}(n)$	60.1	70.4	87.3	90.0*	88.0*	93.0*	91.5	94.7	84.4
<i>Pre-train from scratch</i>										
Linformer [48]	$\mathcal{O}(n)$	/	/	/	/	/	91.2	90.8	93.1	/
Nyströmformer [49]	$\mathcal{O}(n)$	/	/	88.1	/	80.9	88.7	86.3	91.4	/
Ours	$\mathcal{O}(n \log n)$	64.7*	75.1*	88.5*	89.4	86.4	91.3	91.7*	94.8*	85.2*

NPRF-Transformer with RPE can achieve comparable performances with vanilla Transformers and can be trained from scratch for all tasks due to using the low-variance kernels.<sup>6</sup>

## 4 Experiments

In this section, we conduct experiments to verify the effectiveness of our approach on several benchmark datasets covering language pre-training, language modeling, machine translation, and image classification. Then we provide the ablation study and discussions on the design choices. Due to space limitations, detailed description of the experiment settings are presented in Appendix A.

### 4.1 Language Pre-training

We use the BERT-base architecture [9] in our experiments, which consists of 12 Transformer layers. For each layer, the hidden size is set to 768, and the number of attention heads is set to 12. We follow [23] to construct the data corpus and train the model using masked language modeling task. We use the GLUE (General Language Understanding Evaluation) dataset [47] as the downstream tasks to evaluate the performance of the pre-trained models. All codes are implemented based on *fairseq* [28] in *PyTorch* [31]. All models are run on 64 NVIDIA Tesla V100 GPUs with mixed-precision [26].

To show the effectiveness of our proposed NPRF-Transformer with RPE, we choose several competitive baselines in literature, including : Linformer [48], Nyströmformer [49], SMYRF [7], and Fast Clustered Attention (FCA) [46]. All the baselines use the same architecture as ours. The details

<sup>6</sup>The expressive power of NPRF-Transformer with RPE can be weaker than vanilla Transformer as it can only produce *context-agnostic* sharp distribution (from RPE) but may not produce *context-aware* sharp patterns. However, this does not conflict with the observation that NPRF-Transformer with RPE outperforms PRF-Transformer in practice. Although PRF Transformer seems to have more flexibility, its training instability issue hinders the model from learning well.

Table 2: Language model perplexity scores on WikiText-103 validation set. We use \* to indicate the best performance. All the results of the baseline methods are reported in [32].

Model	Perplexity
Vanilla Transformer	33.0
Linear Transformer	38.4
TRF-Transformer	33.6
TRF-Transformer-GATE	31.3
NPRF-Transformer w/ RPE (Ours)	30.6*

about these baselines can be found in Appendix A.1. For all baselines, we report the number in their original papers. We also tried to train the PRF Transformer model from scratch or continue to train a PRF Transformer from the released RoBERTa checkpoint [23]. But all the efforts failed due to the optimization instability issue. For our model, we directly modify the self-attention layer using normalized kernelized attention with RPE and train it from scratch.

The overall comparison results are presented in Table 1 (“/” indicates the GLUE score of the corresponding downstream task is not reported). It can be easily seen that our NPRF-Transformer with RPE outperforms the previous works in terms of the average GLUE score, with a light computational overhead. Beyond the superior performance, it is also worth noting that our model can be stably pre-trained from scratch, which is particularly important in practice.

## 4.2 Language Modeling

We conduct experiments on WikiText-103 language modeling task to demonstrate the effectiveness of our proposed method. We compare our model with the following baselines: 1. Transformer with softmax attention. 2. *Linear Transformer* proposed in [17], which uses kernelized attention with  $\text{elu}(\cdot) + 1$  as its feature map. 3. TRF-Transformer using TRF kernel (called *RFA* in [32]). 4. *TRF-Transformer-GATE* [32], which uses a gating mechanism to further boost performance.

Following [32], the sequence length is set to 512 during both training and evaluation. All models are trained without access to the context from previous mini-batches for a fair comparison. The model architecture consists of 6 decoder layers. The number of attention head is set to 8. The hidden dimension is set to 512. The dimension of feed-forward layer is set to 2048. The dropout ratio and the weight decay are set to 0.1 and 0.01, respectively. The batch size is set to 64. The feature map dimension is set to 64. We use Adam [19] as the optimizer, and set its hyperparameter  $\epsilon$  to  $1e - 6$  and  $(\beta_1, \beta_2)$  to  $(0.9, 0.98)$ . The peak learning rate is set to  $2e - 3$ . The model is trained for 150k steps with a 6k-step warm-up stage followed by an inverse square-root learning rate scheduler. All models are trained on 8 NVIDIA Tesla V100 GPUs.

The results are shown in Table 2. Our NPRF-Transformer with RPE outperforms all the baselines by a large margin, e.g., it achieves a 30.6 perplexity score which is 3.0 lower than the baseline TRF-Transformer and 0.7 lower than TRF-Transformer-GATE. It is worth noting that we mainly make architectural changes and should compare our model with TRF-Transformer. In [32], a set of training tricks (such as gating) are introduced for improving the performance. Our method can be combined with those tricks for further improvements.

## 4.3 Machine Translation

In machine translation, we evaluate our method on the widely used public dataset IWSLT14 German↔English and French↔English. For each language pair, we use a vocabulary of 10K tokens based on a joint source and target byte pair encoding (BPE) [36]. All the experiments use a Transformer encoder-decoder architecture, with a 6-layer encoder and 6-layer decoder. We set the embedding dimension to 512 and the number of heads to 4. For a fair comparison, we set the feature map dimension to 16 in the encoder and 24 in the decoder whenever kernelized attention is used. BLEU [29] is used as the evaluation measure of the model performance. In this small-scale task, we find the optimization for all the model variants is stable, and all models are trained from scratch.

Table 3: Test BLEU scores on machine translation tasks. We use \*/\*\* to indicate the best performance obtained by the standard model / efficient model. “Enc/dec” denotes “encoder/decoder” for short.

Transformer model type	Complexity encoder / decoder	Encoder softmax PRF	Decoder softmax PRF	BLEU			
				de-en	en-de	fr-en	en-fr
Standard enc-dec	$\mathcal{O}(n^2)/\mathcal{O}(n^2)$	✓	✓	34.7*	29.2	40.0	40.2
Standard enc + PRF dec	$\mathcal{O}(n^2)/\mathcal{O}(n)$	✓	✓	34.6	29.3*	40.3*	40.6*
PRF enc-dec	$\mathcal{O}(n)/\mathcal{O}(n)$	✓	✓	32.1	27.6	38.0	38.2
NPRF enc-dec w/ RPE (Ours)	$\mathcal{O}(n \log n)/\mathcal{O}(n \log n)$	✓	✓	34.3**	29.4**	39.9**	40.4**
							36.0**

Table 4: Test accuracy on ImageNet. We use \*/\*\* to indicate the best performance obtained by the standard model / efficient model.

Model	Complexity	Query/key		Attention softmax	ImageNet	
		standard	normalized		Top-1 acc	Top-5 acc
ViT-base[10]	$\mathcal{O}(n^2)$	✓		✓	77.9	/
ViT-large[10]	$\mathcal{O}(n^2)$	✓		✓	76.5	/
DeiT-base	$\mathcal{O}(n^2)$	✓		✓	81.2*	95.0*
PRF DeiT-base (fine-tuned)	$\mathcal{O}(n)$	✓		✓	79.5	94.1
NPRF DeiT-base w/o RPE	$\mathcal{O}(n)$		✓	✓	77.7	93.3
NPRF DeiT-base w/ RPE (Ours)	$\mathcal{O}(n \log n)$		✓	✓	80.9**	94.8**

As the translation task uses an encoder-decoder framework, it is natural to check whether the attention modification (i.e., kernelized attention) can be applied to both encoder and decoder. In [32], the authors only show that using TRF attention in the decoder will not hurt the model performance. But we argue that a long target sequence usually corresponds to a long source sequence in translation, and modifying the attentions in both encoder and decoder should be equally important.

We give a systematic study on the model performance of using PRF in the encoder/decoder and summarize the results shown in Table 3. We first observe that models using PRF kernel in the decoder are comparable with or even slightly better than standard ones (the 2nd line v.s. the 1st line), which is consistent with [32]. The performance improvement may be attributed to regularization effects brought by the randomness in PRF. However, the overall time cost should still be  $\mathcal{O}(n^2)$  as the standard attention is used in the encoder. When applying the kernelized attention to both encoder and decoder, we observe a significant performance drop (the 3rd line v.s. the 1st line). This may indicate that when using more layers of kernelized attention, the model becomes harder to train due to accumulated approximation error through layers. On the contrary, our method can incorporate kernelized attention in both encoder and decoder, achieving the same average BLEU score as the standard Transformer.

#### 4.4 Image Classification on ImageNet

Beyond the natural language tasks, we also extend our study to image classification. We use the DeiT-base [42] as our backbone architecture, which consists of 12 Transformer layers. For each layer, the hidden size is set to 768, and the number of attention heads is set to 12. We set the feature map dimension to 32 whenever kernelized attention is used. Following [10, 42], we benchmark our method on ImageNet-1K [8], which contains 1.28M training images and 50K validation images from 1,000 classes. For evaluation, the top-1/top-5 accuracy on a single crop is reported. For our proposed method, we use the 2-dimensional relative positional encoding developed in [24].

We compare our proposed model with several baseline models using standard attentions, including ViT-base/ViT-large proposed in [10] and the DeiT-base [42]. We also compare our model with a finetuned PRF attention model from DeiT, and an NPRF attention model without RPE. The result is shown in Table 4. First, we can see that our model achieves competitive performance compared to standard attention models (81.2 v.s. 80.9 in terms of top-1 accuracy, 95.0 v.s. 94.8 in terms of top-5 accuracy). Second, we can see that compared with other efficient variants, our model achieves the best performance, and the use of normalized queries/keys and RPE are both helpful.

#### 4.5 More Analyses

We conducted more studies the IWSLT14 German-to-English (De-En) task to ablate our designs.

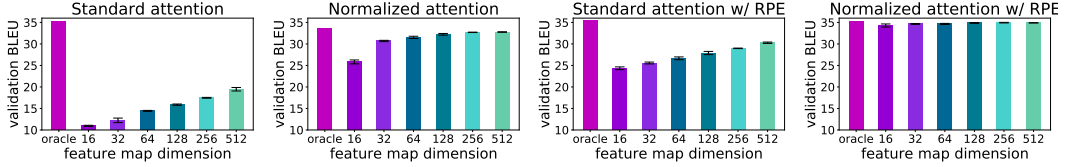


Figure 2: Performance of kernelized attention models converted from well-trained Transformers. “Oracle” represents the BLEU score of the well-trained model for reference.

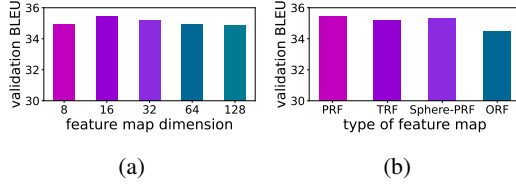


Figure 3: (a). Performance of the NPRF-Transformer with RPE using different feature map dimensions. (b). Performance of the models using different feature map functions.

**Normalized attention is easy to be converted to its kernelized version** We conduct experiments to study whether using normalized attention can practically mitigate the performance drop issue observed in the previous works. We train four model variants: Transformer with standard/normalized attention and with/without RPE. After the training finishes, we replace the attention softmax functions by Equation 5 *without* further finetuning. For each setting, we run with 5 random seeds. Figure 2 summarizes the experiment results in terms of the validation BLEU scores with confidence intervals.

We can see that Transformer with standard attention suffers a considerable performance degradation after the conversion. In contrast, Transformer with normalized attention only suffers a small performance drop. This clearly shows that normalization reduces the approximate error significantly. Interestingly, we observe that RPE *universally* improves the performance of the converted model for both standard and normalized attention. For our NPRF-Transformer with RPE, the feature map dimension is not sensitive any longer, e.g., the converted model only has a 0.5 performance drop when the feature map dimension is only 32.

**Affects of feature map dimensions and other choices of feature map** The dimension of feature map  $\phi$  is a hyper-parameter that balances the accuracy and efficiency. For our NPRF-Transformer with RPE, we train models from scratch with different feature map dimensions and check the validation BLEU. We can see from Figure 3a that the feature map dimension is not sensitive regarding the final performance. Setting the dimensionality to 16 is even a slightly better choice.

Our approach is general which can be applied to any feature map function. The main body of the paper showcases models using the PRF feature map, and here we provide some empirical comparisons with other feature maps. Specifically, we experiment with 1) the TRF feature map defined by Equation 4; 2) the Sphere-PRF feature map, which is designed in [4] as an alternative choice of PRF, where all  $w_i$  in Equation 5 are sampled independently from  $\text{Unif}(\sqrt{d}\mathbb{S}^{d-1})$ ; 3) the ORF feature map, which is also designed in [4] where  $w_1, \dots, w_D$  in Equation 5 are forced to be orthogonal to each other. For all the choices, we train models with normalized kernelized attention and RPE under the same setting as in Section 4.3 and report the best validation BLEU. The results are shown in Figure 3b. We can see that when we normalize the attention and use RPE, all models obtain similar performance.

## 5 Conclusion

In this paper, we propose a novel way to accelerate attention calculation for Transformers with relative positional encoding and achieve  $\mathcal{O}(n \log n)$  time complexity. Our method is built on top of the kernelized attention. Using the fact that relative positional encoding forms a Toeplitz matrix, we mathematically show that kernelized attention with RPE can be calculated efficiently using Fast Fourier Transform (FFT). We further demonstrate the additional benefit of using relative positional encoding from the optimization perspective. As mentioned in the main paper, we will extend the current method to the decoder model in generation tasks and explore more strategies to accelerate attention in the long-sequence regime.

## Acknowledgements

We thank all the anonymous reviewers for their constructive comments. This work was supported by National Key R&D Program of China (2018YFB1402600), Key-Area Research and Development Program of Guangdong Province (No.2019B121204008), BJNSF (L172037) and Beijing Academy of Artificial Intelligence. Project 2020BD006 supported by PKU-Baidu Fund.

## References

- [1] Hangbo Bao, Li Dong, Furu Wei, Wenhui Wang, Nan Yang, Xiaodong Liu, Yu Wang, Jianfeng Gao, Songhao Piao, Ming Zhou, et al. Unilmv2: Pseudo-masked language models for unified language model pre-training. In *International Conference on Machine Learning*, pages 642–652. PMLR, 2020.
- [2] Nicolas Carion, Francisco Massa, Gabriel Synnaeve, Nicolas Usunier, Alexander Kirillov, and Sergey Zagoruyko. End-to-end object detection with transformers. In *European Conference on Computer Vision*, pages 213–229. Springer, 2020.
- [3] Rewon Child, Scott Gray, Alec Radford, and Ilya Sutskever. Generating long sequences with sparse transformers. *arXiv preprint arXiv:1904.10509*, 2019.
- [4] Krzysztof Marcin Choromanski, Valerii Likhoshesterov, David Dohan, Xingyou Song, Andreea Gane, Tamas Sarlos, Peter Hawkins, Jared Quincy Davis, Afroz Mohiuddin, Lukasz Kaiser, David Benjamin Belanger, Lucy J Colwell, and Adrian Weller. Rethinking attention with performers. In *International Conference on Learning Representations*, 2021.
- [5] Patryk Chrabaszcz, Ilya Loshchilov, and Frank Hutter. A downsampled variant of imagenet as an alternative to the cifar datasets. *arXiv preprint arXiv:1707.08819*, 2017.
- [6] Kevin Clark, Urvashi Khandelwal, Omer Levy, and Christopher D Manning. What does bert look at? an analysis of bert’s attention. *ACL 2019*, page 276, 2019.
- [7] Giannis Daras, Nikita Kitaev, Augustus Odena, and Alexandros G Dimakis. Smyrf-efficient attention using asymmetric clustering. *Advances in Neural Information Processing Systems*, 33, 2020.
- [8] Jia Deng, Wei Dong, Richard Socher, Li-Jia Li, Kai Li, and Li Fei-Fei. Imagenet: A large-scale hierarchical image database. In *2009 IEEE conference on computer vision and pattern recognition*, pages 248–255. Ieee, 2009.
- [9] Jacob Devlin, Ming-Wei Chang, Kenton Lee, and Kristina Toutanova. Bert: Pre-training of deep bidirectional transformers for language understanding. In *Proceedings of the 2019 Conference of the North American Chapter of the Association for Computational Linguistics: Human Language Technologies, Volume 1 (Long and Short Papers)*, pages 4171–4186, 2019.
- [10] Alexey Dosovitskiy, Lucas Beyer, Alexander Kolesnikov, Dirk Weissenborn, Xiaohua Zhai, Thomas Unterthiner, Mostafa Dehghani, Matthias Minderer, Georg Heigold, Sylvain Gelly, Jakob Uszkoreit, and Neil Houlsby. An image is worth 16x16 words: Transformers for image recognition at scale. In *International Conference on Learning Representations*, 2021.
- [11] Robert M Gray. *Toeplitz and circulant matrices: A review*. now publishers inc, 2006.
- [12] Matej Grcić, Ivan Grubišić, and Siniša Šegvić. Densely connected normalizing flows. *arXiv preprint arXiv:2106.04627*, 2021.
- [13] Anmol Gulati, James Qin, Chung-Cheng Chiu, Niki Parmar, Yu Zhang, Jiahui Yu, Wei Han, Shibo Wang, Zhengdong Zhang, Yonghui Wu, et al. Conformer: Convolution-augmented transformer for speech recognition. *Proc. Interspeech 2020*, pages 5036–5040, 2020.
- [14] Pengcheng He, Xiaodong Liu, Jianfeng Gao, and Weizhu Chen. Deberta: Decoding-enhanced bert with disentangled attention. In *International Conference on Learning Representations*, 2021.
- [15] Jonathan Ho, Nal Kalchbrenner, Dirk Weissenborn, and Tim Salimans. Axial attention in multidimensional transformers, 2019.
- [16] Jungo Kasai, Hao Peng, Yizhe Zhang, Dani Yogatama, Gabriel Ilharco, Nikolaos Pappas, Yi Mao, Weizhu Chen, and Noah A. Smith. Finetuning pretrained transformers into rnns, 2021.

- [17] Angelos Katharopoulos, Apoorv Vyas, Nikolaos Pappas, and François Fleuret. Transformers are rnns: Fast autoregressive transformers with linear attention. In *International Conference on Machine Learning*, pages 5156–5165. PMLR, 2020.
- [18] Guolin Ke, Di He, and Tie-Yan Liu. Rethinking positional encoding in language pre-training. In *International Conference on Learning Representations*, 2021.
- [19] Diederik P Kingma and Jimmy Ba. Adam: A method for stochastic optimization. In *ICLR (Poster)*, 2015.
- [20] Diederik P Kingma, Tim Salimans, Ben Poole, and Jonathan Ho. Variational diffusion models. *arXiv preprint arXiv:2107.00630*, 2021.
- [21] Nikita Kitaev, Lukasz Kaiser, and Anselm Levskaya. Reformer: The efficient transformer. In *International Conference on Learning Representations*, 2019.
- [22] Taku Kudo and John Richardson. Sentencepiece: A simple and language independent subword tokenizer and detokenizer for neural text processing. In *Proceedings of the 2018 Conference on Empirical Methods in Natural Language Processing: System Demonstrations*, pages 66–71, 2018.
- [23] Yinhan Liu, Myle Ott, Naman Goyal, Jingfei Du, Mandar Joshi, Danqi Chen, Omer Levy, Mike Lewis, Luke Zettlemoyer, and Veselin Stoyanov. Roberta: A robustly optimized bert pretraining approach. *arXiv preprint arXiv:1907.11692*, 2019.
- [24] Ze Liu, Yutong Lin, Yue Cao, Han Hu, Yixuan Wei, Zheng Zhang, Stephen Lin, and Baining Guo. Swin transformer: Hierarchical vision transformer using shifted windows. *arXiv preprint arXiv:2103.14030*, 2021.
- [25] Ilya Loshchilov and Frank Hutter. Fixing weight decay regularization in adam, 2018.
- [26] Paulius Micikevicius, Sharan Narang, Jonah Alben, Gregory Diamos, Erich Elsen, David Garcia, Boris Ginsburg, Michael Houston, Oleksii Kuchaiev, Ganesh Venkatesh, and Hao Wu. Mixed precision training, 2018.
- [27] Sharan Narang, Hyung Won Chung, Yi Tay, William Fedus, Thibault Fevry, Michael Matena, Karishma Malkan, Noah Fiedel, Noam Shazeer, Zhenzhong Lan, et al. Do transformer modifications transfer across implementations and applications? *arXiv preprint arXiv:2102.11972*, 2021.
- [28] Myle Ott, Sergey Edunov, Alexei Baevski, Angela Fan, Sam Gross, Nathan Ng, David Grangier, and Michael Auli. fairseq: A fast, extensible toolkit for sequence modeling. In *Proceedings of NAACL-HLT 2019: Demonstrations*, 2019.
- [29] Kishore Papineni, Salim Roukos, Todd Ward, and Wei-Jing Zhu. Bleu: a method for automatic evaluation of machine translation. In *Proceedings of the 40th annual meeting on association for computational linguistics*, pages 311–318. Association for Computational Linguistics, 2002.
- [30] Niki Parmar, Ashish Vaswani, Jakob Uszkoreit, Lukasz Kaiser, Noam Shazeer, Alexander Ku, and Dustin Tran. Image transformer. In *International Conference on Machine Learning*, pages 4055–4064. PMLR, 2018.
- [31] Adam Paszke, Sam Gross, Francisco Massa, Adam Lerer, James Bradbury, Gregory Chanan, Trevor Killeen, Zeming Lin, Natalia Gimelshein, Luca Antiga, et al. Pytorch: An imperative style, high-performance deep learning library. *Advances in Neural Information Processing Systems*, 32:8026–8037, 2019.
- [32] Hao Peng, Nikolaos Pappas, Dani Yogatama, Roy Schwartz, Noah Smith, and Lingpeng Kong. Random feature attention. In *International Conference on Learning Representations*, 2021.
- [33] Jiezhong Qiu, Hao Ma, Omer Levy, Wen-tau Yih, Sinong Wang, and Jie Tang. Blockwise self-attention for long document understanding. In *Proceedings of the 2020 Conference on Empirical Methods in Natural Language Processing: Findings*, pages 2555–2565, 2020.
- [34] Alec Radford, Jeff Wu, Rewon Child, David Luan, Dario Amodei, and Ilya Sutskever. Language models are unsupervised multitask learners. 2019.
- [35] Colin Raffel, Noam Shazeer, Adam Roberts, Katherine Lee, Sharan Narang, Michael Matena, Yanqi Zhou, Wei Li, and Peter J. Liu. Exploring the limits of transfer learning with a unified text-to-text transformer, 2020.

- [36] Rico Sennrich, Barry Haddow, and Alexandra Birch. Neural machine translation of rare words with subword units. In *Proceedings of the 54th Annual Meeting of the Association for Computational Linguistics (Volume 1: Long Papers)*, pages 1715–1725, 2016.
- [37] Rico Sennrich, Barry Haddow, and Alexandra Birch. Neural machine translation of rare words with subword units. In *ACL*, 2016.
- [38] Peter Shaw, Jakob Uszkoreit, and Ashish Vaswani. Self-attention with relative position representations. *arXiv preprint arXiv:1803.02155*, 2018.
- [39] Yang Song, Conor Durkan, Iain Murray, and Stefano Ermon. Maximum likelihood training of score-based diffusion models. *arXiv e-prints*, pages arXiv–2101, 2021.
- [40] Christian Szegedy, Vincent Vanhoucke, Sergey Ioffe, Jon Shlens, and Zbigniew Wojna. Rethinking the inception architecture for computer vision. In *Proceedings of the IEEE Conference on Computer Vision and Pattern Recognition*, pages 2818–2826, 2016.
- [41] Yi Tay, Mostafa Dehghani, Dara Bahri, and Donald Metzler. Efficient transformers: A survey, 2020.
- [42] Hugo Touvron, Matthieu Cord, Matthijs Douze, Francisco Massa, Alexandre Sablayrolles, and Hervé Jégou. Training data-efficient image transformers & distillation through attention, 2021.
- [43] Trieu H Trinh and Quoc V Le. A simple method for commonsense reasoning. *arXiv preprint arXiv:1806.02847*, 2018.
- [44] Yao-Hung Hubert Tsai, Shaojie Bai, Makoto Yamada, Louis-Philippe Morency, and Ruslan Salakhutdinov. Transformer dissection: An unified understanding for transformer’s attention via the lens of kernel. In *Proceedings of the 2019 Conference on Empirical Methods in Natural Language Processing and the 9th International Joint Conference on Natural Language Processing (EMNLP-IJCNLP)*, pages 4335–4344, 2019.
- [45] Ashish Vaswani, Noam Shazeer, Niki Parmar, Jakob Uszkoreit, Llion Jones, Aidan N Gomez, Łukasz Kaiser, and Illia Polosukhin. Attention is all you need. In *Advances in neural information processing systems*, pages 5998–6008, 2017.
- [46] Apoorv Vyas, Angelos Katharopoulos, and François Fleuret. Fast transformers with clustered attention. *Advances in Neural Information Processing Systems*, 33, 2020.
- [47] Alex Wang, Amanpreet Singh, Julian Michael, Felix Hill, Omer Levy, and Samuel R. Bowman. Glue: A multi-task benchmark and analysis platform for natural language understanding. 2019. In the Proceedings of ICLR.
- [48] Sinong Wang, Belinda Z. Li, Madian Khabsa, Han Fang, and Hao Ma. Linformer: Self-attention with linear complexity, 2020.
- [49] Yunyang Xiong, Zhanpeng Zeng, Rudrasis Chakraborty, Mingxing Tan, Glenn Fung, Yin Li, and Vikas Singh. Nyströmformer: A nyström-based algorithm for approximating self-attention. In *Proceedings of the AAAI Conference on Artificial Intelligence*, 2021.
- [50] Zhilin Yang, Zihang Dai, Yiming Yang, Jaime Carbonell, Russ R Salakhutdinov, and Quoc V Le. Xlnet: Generalized autoregressive pretraining for language understanding. *Advances in Neural Information Processing Systems*, 32:5753–5763, 2019.
- [51] Yukun Zhu, Ryan Kiros, Rich Zemel, Ruslan Salakhutdinov, Raquel Urtasun, Antonio Torralba, and Sanja Fidler. Aligning books and movies: Towards story-like visual explanations by watching movies and reading books. In *Proceedings of the IEEE international conference on computer vision*, pages 19–27, 2015.

## A Experiments

### A.1 Language Pre-training

**Baselines.** To show the effectiveness of our proposed NPRF-Transformer with RPE, we choose several competitive baselines in literature covering Low-Rank Approximation based Attention, Sparse Attention and Kernelized Attention, including : 1. *Linformer* proposed in [48], which projects the length dimension of keys and values to lower-dimensional representations ( $N \rightarrow K$ ) and induces  $\mathcal{O}(NK)$  time complexity; 2. *Nyströmformer* proposed in [49], which uses Nyström approximation and reduces the time complexity to  $\mathcal{O}(NM)$ , where  $M(M \ll N)$  is the number of landmarks of Nyström method; 3. *SMYRF* proposed in [7], which uses Locality Sensitive Hashing (LSH) and newly defined Asymmetric transformation to produce balanced query-key clusters, introducing  $\mathcal{O}(N \log N)$  time complexity; 4. *Fast Clustered Attention (FCA)* proposed in [46], which first groups queries into clusters and computes attention for the centroids, inducing  $\mathcal{O}(NC)$  time complexity with  $C$  denoting the number of clusters.

**Pre-training.** Following [23], we collect five English-language corpora of varying sizes and domains, totaling over 160GB of uncompressed text. The pre-training corpora consist of Bookcorpus[51] and English wikipedia, CC-News<sup>7</sup>, OpenWebText<sup>8</sup> and Stories[43]. Detailed description of these corpora can be found in [23]. We follow [23] to conduct a couple of consecutive pre-processing steps: segmenting documents into sentences by Spacy<sup>9</sup>, normalizing, lower-casing, and tokenizing the texts by using SentencePiece [22].

We use masked language modeling as the objective of pre-training. We train the models for 1000k steps where the batch size is 2048 and the maximum sequence length is 512. The masked probability is set to 0.15, and we replace 80% of the masked positions with [MASK], 10% with randomly sampled words, and keep the remaining 10% unchanged. We use Adam [19] as the optimizer, and set its hyperparameter  $\epsilon$  to  $1e - 6$  and  $(\beta_1, \beta_2)$  to  $(0.9, 0.999)$ . The peak learning rate is set to  $2e - 4$  with a 20k-step warm-up stage. After the warm-up stage, the learning rate decays linearly to zero. We set the dropout probability to 0.1, gradient clip norm to 1.0, and weight decay to 0.01. All models are trained on 64 NVIDIA Tesla V100 GPUs. The pre-training setting details are listed in Table 5.

**Fine-tuning.** We use the GLUE (General Language Understanding Evaluation) dataset [47] as the downstream tasks to evaluate the performance of the pre-trained models. Particularly, we use nine tasks in GLUE, including CoLA, RTE, MRPC, STS, SST, QNLI, QQP, and MNLI. For the evaluation metrics, we report Matthews correlation for CoLA, Pearson correlation for STS-B, and accuracy for other tasks. We use the same optimizer (Adam) as in pre-training. Following previous works, we search the learning rates during the fine-tuning for each downstream task. For a fair comparison, we do not apply any tricks for fine-tuning. Each configuration will be run five times with different random seeds, and the median of these five results on the development set will be used as the performance of one configuration. We report the best score over all configurations. The fine-tuning setting details are listed in Table 5.

### A.2 Language Modeling

**Baselines.** We compare our model with the following baselines: 1. *Transformer* with softmax attention. 2. *Linear Transformer* proposed in [17], which uses kernelized attention with  $\text{elu}(\cdot) + 1$  as its feature map. 3. TRF-Transformer using TRF kernel (called *RFA* in [32]). 4. *TRF-Transformer-GATE* [32], which uses a gating mechanism to further boost performance.

**Settings.** Following [32], the sequence length is set to 512 during both training and evaluation. All models are trained without access to the context from previous mini-batches for a fair comparison. The model architecture consists of 6 decoder layers. The number of attention head is set to 8. The hidden dimension is set to 512. The dimension of feed-forward layer is set to 2048. The dropout ratio

<sup>7</sup><http://web.archive.org/save/http://commoncrawl.org/2016/10/newsdataset-available>

<sup>8</sup><http://web.archive.org/save/http://Skylion007.github.io/OpenWebTextCorpus>

<sup>9</sup><https://spacy.io>

<sup>10</sup>We use five for the top four high-resource tasks, MNLI-m-mm, QQP, and QNLI, to save the fine-tuning costs. Ten is used for other tasks.

Table 5: Hyperparameters used in the Language Pre-training task.

	Pre-training	Fine-tuning
<i>Model Configuration</i>		
<b>Layers</b>	12	
<b>Hidden Representation</b>	768	
<b>Feed-Forward Layer</b>	3072	
<b>Heads</b>	12	
<i>Hyperparameters</i>		
<b>Max Steps</b>	1000k	-
<b>Max Epochs</b>	-	5 or $10^{10}$
<b>Learning Rate</b>	2e-4	{5e-6, 1e-5, 2e-5, 3e-5, 4e-5}
<b>Warm-up Ratio</b>	2%	6%
<b>Learning Rate Decay</b>	Linear	Linear
<b>Batch Size</b>	2048	16 or 32
<b>Sequence Length</b>	512	512
<b>Adam <math>\epsilon</math></b>	1e-6	1e-6
<b>Adam(<math>\beta_1, \beta_2</math>)</b>	(0.9, 0.999)	(0.9, 0.98)
<b>Clip Norm</b>	1.0	1.0
<b>Dropout</b>	0.1	0.1
<b>Weight Decay</b>	0.01	0.01

and the weight decay are set to 0.1 and 0.01, respectively. The batch size is set to 64. The feature map dimension is set to 64. We use Adam [19] as the optimizer, and set its hyperparameter  $\epsilon$  to  $1e - 6$  and  $(\beta_1, \beta_2)$  to  $(0.9, 0.98)$ . The peak learning rate is set to  $2e - 3$ . The model is trained for 150k steps with a 6k-step warm-up stage followed by an inverse square-root learning rate scheduler. All models are trained on 8 NVIDIA Tesla V100 GPUs.

### A.3 Machine Translation

We train the models on the widely used public dataset IWSLT14 German↔English and French↔English. For each language pair, we use a vocabulary of 10K tokens based on a joint source and target byte pair encoding (BPE) [37]. All the experiments use a Transformer encoder-decoder architecture, with a 6-layer encoder and a 6-layer decoder. We set the embedding dimension to 512 and the number of heads to 4. When kernelized attention is used, the feature map dimension is set to 16 in the encoder and 24 in the decoder. For all the models, label smoothed cross entropy is used as the objective function by setting  $\epsilon = 0.1$  [40], and we apply dropout with a ratio 0.3. The batch size is set to be 8192 tokens. When we decode translation results from the model during inference, we set beam size as 5 and the length penalty as 1.2. All the models are trained for 50k steps with 4000 warm up steps and a peak learning rate of  $5e - 4$ , and an inverse square root learning rate scheduler is used after the warm-up stage. All the models are trained with the Adam optimizer [19], in which hyperparameter  $(\beta_1, \beta_2)$  is to be  $(0.9, 0.98)$  following [45]. BLEU [29] is used as the evaluation measure of the model performance, and we report the BLEU score of a single checkpoint, without using checkpoint averaging. All models are trained on 4 NVIDIA Tesla V100 GPUs.

### A.4 Image Classification

**Baselines.** In the image classification task, we compare our proposed model with several Transformer-based models using softmax attention, including: 1. *ViT* proposed in [10], which first introduces the idea of handling images as sequences of fixed-sized patches and feeding them into Transformer to perform classification; 2. *DeiT* proposed in [42], which largely improves the performance of ViT using strong data augmentation and knowledge distillation<sup>11</sup>.

<sup>11</sup>For simplicity, in our model and all baseline models, knowledge distillation is not used.

**Training details.** Our training settings mostly follow [42]. We train all the models on the training set of ImageNet-1K [8]. We adopt a default input image resolution of  $224 \times 224$  without finetuning the model on a higher resolution. When training NPRF-DeiT from scratch, we employ the AdamW [25] optimizer for 450 epochs using a cosine decay learning rate scheduler with 20 epochs of linear warm-up. When finetuning PRF-DeiT from DeiT with softmax attention, we employ the AdamW optimizer for 100 epochs using a cosine decay learning rate scheduler with 6 epochs of linear warm-up. For the hyperparameters of the optimizer, we set  $\epsilon$  to  $1e - 8$  and  $(\beta_1, \beta_2)$  to  $(0.9, 0.999)$ . Label smoothed cross entropy is used as the objective function by setting  $\epsilon = 0.1$  [40]. A batch size of 1024, an initial learning rate of  $1e - 5$  and a weight decay of 0.05 are used. We employ all the data augmentation and regularization strategies of [42]. Following [24], we perform image classification by applying a global average pooling layer on the output of the last layer, followed by a linear classifier. All models are trained on 8 NVIDIA Tesla V100 GPUs.

## A.5 Image Generation

We additionally conduct experiments on the ImageNet32 image generation task to demonstrate the effectiveness of our proposed method in the long-sequence regime [5]. In this task, the sequence length is 3072.

**Baselines.** In this task, we compare our proposed NPRF-Transformer with several Transformer-based models as well as several other strong baselines, including Image Transformer [30], PRF-Transformer (called Performer in [4]); ScoreFlow [39], VDM [20] and DenseFlow [12].

**Training details.** We train a 6-layer NPRF-Transformer with RPE. For each layer, the hidden size is set to 512, and the number of attention heads is set to 8. When training our model, we use a batch size of 64. We use Adam [19] as the optimizer, and set its hyperparameter  $\epsilon$  to  $1e - 6$  and  $(\beta_1, \beta_2)$  to  $(0.9, 0.98)$ . We set the dropout ratio and the weight decay to 0.1 and 0.01, respectively. The feature map dimension is set to 32 whenever kernelized attention is used. The peak learning rate is set to  $5e - 4$ . We use the BPD (bits per dim) to evaluate the performance of the models.

**Results.** The result is shown in Table 6. It’s easy to see that our NPRF-Transformer with RPE outperforms other Transformer-based models by a large margin. Specifically, it outperforms PRF-Transformer by 0.36 points, which shows that our method largely improves the performance kernelized attention on large-scale dataset. Besides, our NPRF-Transformer with RPE also achieves competitive performance compared with other strong baselines, and is almost on par with DenseFlow, the state-of-the-art model for image generation. These results clearly demonstrate the effectiveness of our proposed method in long-sequence regime.

Table 6: Bits per Dimension (Bits/Dim) on ImageNet32. “\*\*” indicates the best model and “\*\*\*” indicates the best Transformer-based model.

Method	BPD
ScoreFlow [39]	3.76
VDM [20]	3.72
DenseFlow [12]	3.63*
Image Transformer [30]	3.77
PRF-Transformer	4.04
NPRF-Transformer with RPE (Ours)	3.68**

## B Proofs

### B.1 Proof of Proposition 1

*Proof.* The proof is done by contradiction.

Equation 7 implies

$$\exp(\alpha_{ij}^{rel} - \alpha_{ij}^{vanilla}) = \frac{\sum_{k=1}^n \exp(\alpha_{ik}^{rel})}{\sum_{k=1}^n \exp(\alpha_{ik}^{vanilla})}, \forall i, j. \quad (15)$$

Thus,  $\alpha_{ij}^{rel} - \alpha_{ij}^{vanilla}$  only depends on  $i$ , and we assume  $\alpha_{ij}^{rel} - \alpha_{ij}^{vanilla} = \beta_i$ .

Let  $X = [x_1^\top, \dots, x_n^\top]^\top \in \mathbb{R}^{n \times d}$ ,  $B = \{b_{i-j}\}_{i,j=1}^n$ ,  $\beta = [\beta_1, \dots, \beta_n]^\top$ . Then we obtain

$$\frac{1}{\sqrt{d}} X \left( W_{rel}^Q (W_{rel}^K)^\top - W_{vanilla}^Q (W_{vanilla}^K)^\top \right) X^\top + B = \beta \mathbf{1}^\top \quad (16)$$

$$\Rightarrow B = \frac{1}{\sqrt{d}} X \left( W_{vanilla}^Q (W_{vanilla}^K)^\top - W_{rel}^Q (W_{rel}^K)^\top \right) X^\top + \beta \mathbf{1}^\top. \quad (17)$$

Note that  $\text{rank} \left( X \left( W_{vanilla}^Q (W_{vanilla}^K)^\top - W_{rel}^Q (W_{rel}^K)^\top \right) X^\top \right) \leq d$ ,  $\text{rank} (\beta \mathbf{1}^\top) \leq 1$ , thus the above equation implies  $\text{rank}(B) \leq d + 1$ , which cannot hold if  $B$  is full-rank since  $n > d + 1$ .  $\square$

### B.2 Proof of Theorem 3

*Proof.* By definition we have

$$A = \left( \frac{\exp(qk_j^\top)}{\sum_{j'=1}^n \exp(qk_{j'}^\top)} \right)_{j=1}^n; \hat{A} = \left( \frac{\phi(q)\phi(k_j)^\top}{\sum_{j'=1}^n \phi(q)\phi(k_{j'})^\top} \right)_{j=1}^n. \quad (18)$$

For fixed  $q$  and  $k$  and any  $\varepsilon > 0$ , applying Chebyshev's Inequality and lemma 2 we obtain

$$\Pr(|\exp(qk^\top) - \phi(q)\phi(k)^\top| \geq \varepsilon \exp(qk^\top)) \leq \frac{\exp(\|x+y\|^2)(1-\exp(-\|x+y\|^2))}{m\varepsilon^2} \quad (19)$$

$$\leq \frac{\exp(\|x+y\|^2)}{m\varepsilon^2} \quad (20)$$

$$\leq \frac{\exp(2\|x\|^2 + 2\|y\|^2)}{m\varepsilon^2} \quad (21)$$

$$\leq \frac{\exp(4R^2)}{m\varepsilon^2}. \quad (22)$$

Applying union bound for  $(q, k_1), \dots, (q, k_n)$ , and setting  $m = \frac{n \exp(4R^2)}{\varepsilon^2 \delta}$  we obtain

$$\Pr(\exists j, |\exp(q \cdot k_j) - \phi(q) \cdot \phi(k_j)| \geq \varepsilon \exp(q \cdot k_j)) \leq \frac{n \exp(4R^2)}{m \varepsilon^2} = \delta. \quad (23)$$

Assume  $\forall j, |\exp(qk_j^\top) - \phi(q)\phi(k_j)^\top| < \varepsilon \exp(qk_j^\top)$ . Then  $\forall j$

$$\frac{1-\varepsilon}{1+\varepsilon} \cdot \frac{\exp(qk_j^\top)}{\sum_{j'=1}^n \exp(qk_{j'}^\top)} < \frac{\phi(q)\phi(k_j^\top)}{\sum_{j'=1}^n \phi(q)\phi(k_{j'})^\top} < \frac{1+\varepsilon}{1-\varepsilon} \cdot \frac{\exp(qk_j^\top)}{\sum_{j'=1}^n \exp(qk_{j'}^\top)} \quad (24)$$

$$\Rightarrow \left| \frac{\phi(q)\phi(k_j)^\top}{\sum_{j'=1}^n \phi(q)\phi(k_{j'})^\top} - \frac{\exp(qk_j^\top)}{\sum_{j'=1}^n \exp(qk_{j'}^\top)} \right| < \frac{2\varepsilon}{1-\varepsilon} \cdot \frac{\exp(qk_j^\top)}{\sum_{j'=1}^n \exp(qk_{j'}^\top)} \quad (25)$$

$$\Rightarrow \|A - \hat{A}\|_1 < \frac{2\varepsilon}{1-\varepsilon} < 4\varepsilon. \quad (26)$$

Therefore,  $\Pr(\|A - \hat{A}\|_1 \geq 4\varepsilon) \leq \delta$ , which completes the proof.  $\square$